Krzysztof Okoń[1], Rafał Kawa[2]

Microvascular Network in Renal Carcinomas. Quantitative and Tissue Microarray Immunohistochemical Study

[1]Department of Pathomorphology, Collegium Medicum, Jagiellonian University, Kraków
[2]Institute of Computer Science, Jagiellonian University, Kraków

The aim of the study was to investigate differences in microvessels between renal tumors. The material consisted of 97 clear cell carcinomas (CCRCC), 20 papillary carcinomas (PapRCC), 33 chromophobe carcinomas and 15 oncocytomas (RO). The endothelia were stained immunohistochemically for CD34 antigen. The vascular features were analyzed with the AnalySIS image processing system. The stains for VEGF, GLUT-1 and Ki67 were performed on tissue microarrays. The mean microvascular density (MVD) was 163.62 profiles/mm^2 and microvascular area (MVA) was 3.75%. The highest values were seen in CCRCC and the lowest in PapRCC. The size and shape parameters of the individual vessels were also different between the tumors under consideration. The tumor diameter, MVD and MVA were inversely correlated, the relationship being the strongest for RO. The minimum spanning tree parameters were different between histological types, especially between CCRCC and PapRCC. The mean fractal dimension was 1.32, and similar in all cases. VEGF, Ki67 and GLUT-1 expression was the highest in CCRCC, and lowest in RO. The vascular parameters were correlated with Ki67, GLUT-1 VEGF expression, tumor grade, and inversely correlated with tumor diameter. The relationships in each tumor type were slightly different.

Introduction

Angiogenesis (AG), i.e. the formation of small blood vessels, occurs during ontogenesis, but under normal conditions does not take place in an adult human. On the other hand, AG participates in various pathological processes, such as wound healing or organization of inflammatory exudate. AG is indispensable for the development of cancers. Only very early tumors, few millimeters in size, may be supplemented by diffusion from their neighborhood. Acquiring the ability to induce AG is necessary for tumor progression. In some diseases, such as breast carcinoma, the density of the vascular network may be an independent prognostic factor [3, 4, 21]. Clear cell renal carcinomas are known for a very intimate relationship between tumor cells and vessels, but this phenomenon is not so striking in other histologic types. We expected to see important differences in microvascular network between different types of renal tumors and the aim of the study was to examine these relationships.

Material and Methods

The material consisted of renal tumors diagnosed in our institution from 1992 to 2005. The material was formalin fixed, paraffin embedded by routine protocols. From the tissue blocks, 3μm sections were prepared and stained with hematoxylin-eosin. Cases with extensive necrosis, cystic tumors with tiny foci of neoplastic epithelium and secondary tumors were excluded from consideration. All cases were reclassified according to the WHO system [9]. From the bulk of over 700 cases, well preserved and unambiguously diagnosed papillary carcinomas, chromophobe carcinomas and oncocytomas were selected for the study, as well as a randomly chosen set of unambiguous clear cell carcinomas.

Hematoxylin-eosin sections were reviewed and in each case a section was selected that would contain representative and well-preserved carcinoma tissue. Selected paraffin blocks served for preparing 3μm-thick sections for CD34 stain and for constructing tissue microarrays for the other stains using a Tissue MicroArrayer MTA-1 (Beecher

Instruments Inc., WI, USA). From each donor block, three 0.6mm cylinders were cut. The acceptor paraffin blocks were prepared making note of the location of each cylinder, and 3 μm-thick sections were prepared.

For immunohistochemistry, the standard protocol was used. Briefly, the slides were dewaxed, rehydrated and incubated in 3% peroxide solution for 10 minutes to block endogenous peroxidase activity. Antigen retrieval was carried out by microwaving in citrate buffer (pH 6.0) or EDTA (pH 8.0) for 3x5 minutes at 750 W. The primary antibodies are shown in Table 1. The ENVISION + (DAKO, Denmark) detection system was used. It consists of several goat anti-mouse antibody molecules attached to a dextran backbone coupled with horseradish peroxidase, and allows for high signal-low background reactions. 3-amino-9-ethylcarbasole (DAKO, Denmark) was used as the chromogen. The slides were counterstained with Mayer hematoxylin (DAKO, Denmark). The processing was done using the DAKO Autostainter device (DAKO, Denmark).

The pictures from CD34 stained slides were taken with an Olympus BX41 microscope with an Olympus 10x UPlanApo lens. Digital photographs of 10 consecutive non-overlapping fields of vision along a serpentine way were taken. The areas containing only well-preserved neoplastic tissue were chosen. The size of a single picture

TABLE 1
Antibodies used in the study

	Manufacturer	Clone	Antigen retrieval	Dilution	Incubation time
CD34	DAKO	QBEnd10	citrate	1:25	30 minutes
VEGF-A	Santa Cruz	(polyclonal)	EDTA	1:100	60 minutes
GLUT-1	DAKO	(polyclonal)	citrate	1:200	30 minutes
Ki67	Immunotech	MIB-1	citrate	Stock	30 minutes

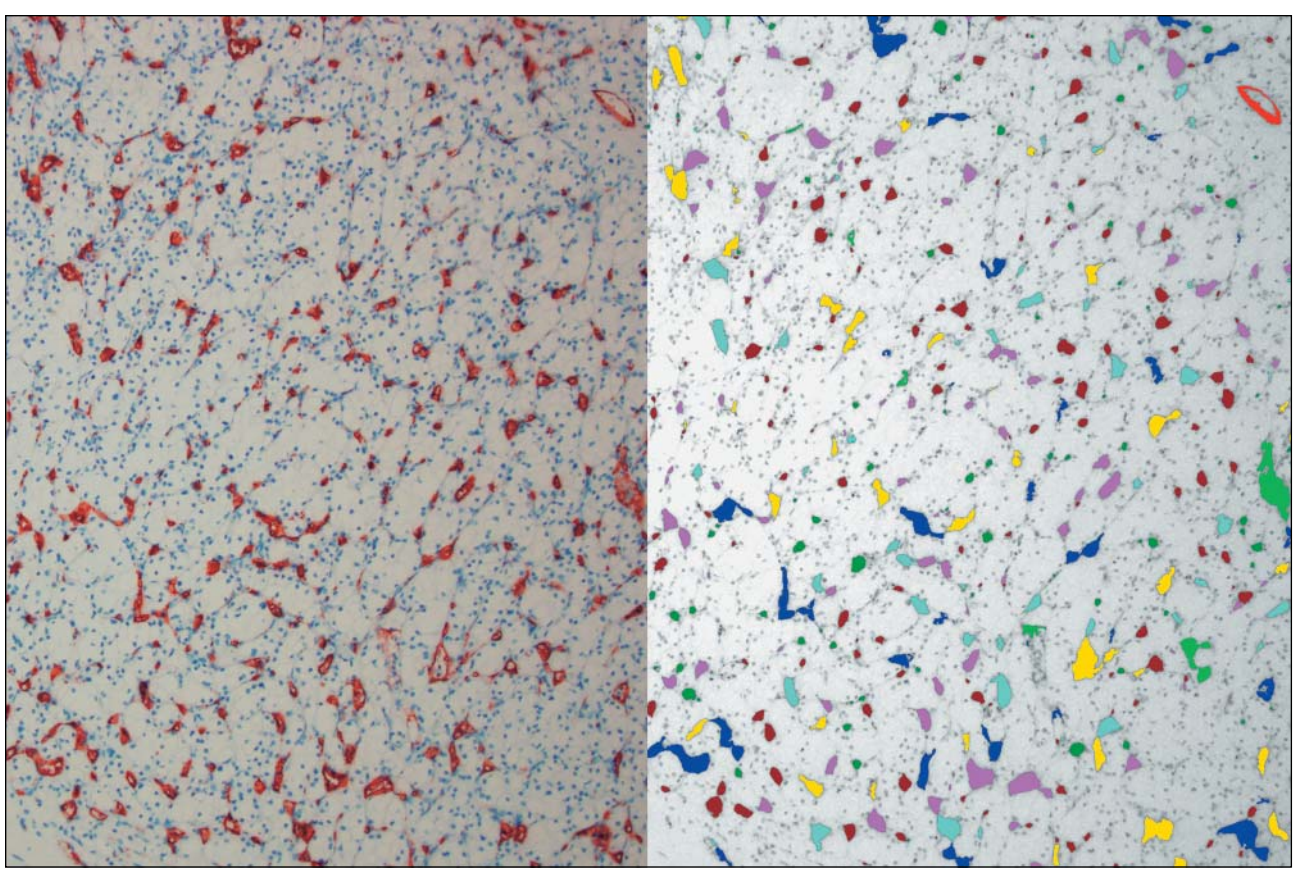

Fig. 1. Example of recognition of vascular profiles - original image (left panel) and transformed image (right panel). The recognized vessels are colored for demonstration purpose only. Lens magnification 10x.

TABLE 2
Diagnoses of the tumors under study

	N	%
Clear Cell Carcinoma	97	58.79
Papillary Carcinoma	20	12.12
Chromophobe Carcinoma	33	20.00
Oncocytoma	15	9.09

where: N is the number of cases, RCC is renal cell carcinoma

was 1.75x1.32mm (2.31 mm^2), represented by 4080x3072 (12 533 760) pixels. The collected pictures were subject to further processing using an application designed by one of us (KO) on the basis of a commercial image analysis system (Analysis pro v. 3.2, Soft Imaging System GmbH, Munster, Germany). This application performed filtering and automatic thresholding, allowing for classification of the picture into vascular profiles and background (Fig. 1). The performance of the program was tested on selected images from the dataset, comparing the program results with the visible, CD34 positive vessels. For this testing, images of several tumors with different diagnoses were used. The obtained vessels were saved as individual bitmaps and at the same time, planimetric measurements were done. The parameters saved were: surface area, minimum and maximum diameter, perimeter, coordinates of the vessel profile and two form factors defined as:

Ellipticity = D_{min} / D_{max}

$SF= L^2/4\pi S$

where:

D_{min} and D_{max} are the minimum and maximum diameter, respectively

L is the perimeter

S is the surface area

The vascular density (MVD) was expressed as the number of vascular profiles per mm^2. The vascular area percentage (MVA) was calculated as the total area of vascular profiles per the total area of the examined images.

To calculate the fractal dimensions of the vessel profiles, the individual bitmaps of the vessel profiles were processed with a set of programs written by RK (used in the previous investigation [40]). The spatial relationships of the vessels were estimated using minimal spanning trees (MST). The coordinates of centers of gravity of each vessel in an image were read by the program developed by KO, and a fully connected, weighted graph was constructed, with distances serving as weights. Then, the procedure of MST construction was called, adapted from the code published by the Association for Computing Machinery Inc. and V.K.M. Whitney [47]. From each MST, the sum of the lengths of the edges (MSTsum), mean of the lengths of the edges (MSTmean), standard deviation of the lengths of the edges (MSTsd), maximum and minimum of the lengths of the edges (MSTmax, MSTmin) were recorded.

The assessment of VEGF-A and GLUT-1 staining was done semiquantitatively, scoring from 0 to 3. Ki67 staining was assessed by counting positive nuclei in individual tissue cores. The tissue microarray results were averaged across the cores belonging to a given case. The results of scoring were introduced into an Excel spreadsheet (Microsoft Corp. USA), in which the relationships between tissue core location and case number were kept.

The Kruskal-Wallis ANOVA, one way ANOVA, χ^2 test, Spearman`s R correlations coefficient, Pearson`s r correlations coefficient, test of the significance of differences between two correlation coefficients in two samples, and discriminant function analysis were used, if appropriate. The statistical analysis was performed with Statistica 7.1 (Statsoft, Tulsa, USA). The significance level was set to 0.05.

Results

The material under study consisted of 165 renal tumors, originating from 69 females and 96 males. The mean age of the patients was 61.19 (range 26 to 89). The diagnoses are

TABLE 3
Geometric parameters of the individual vessels by histologic types

	Area [μm²]		Min diameter [μm]		Max diameter [μm]		Perimeter [μm]		SF		Ellipticity	
	mean	SD	mean	SD	mean	SD	mean	SD	mean	SD	mean	SD
Clear Cell carcinoma	228.65	511.48	12.74	8.91	28.25	23.43	80.53	84.83	0.49	0.22	2.62	1.57
Papillary carcinoma	198.94	860.79	11.81	8.76	24.75	20.07	76.84	119.52	0.46	0.21	2.51	1.39
Chromophobe carcinoma	261.48	793.97	12.89	9.92	30.21	27.16	84.49	105.41	0.50	0.22	2.79	1.79
Oncocytoma	174.99	256.95	11.68	6.72	24.26	16.38	71.05	68.55	0.50	0.23	2.41	1.27

where: SD is standard deviation, SF is shape factor

TABLE 4
Vascular density parameters by diagnoses

	MVD				MVA			
	mean	min	max	SD	mean	min	max	SD
Clear Cell carcinoma	178.15	45.02	489.18	95.91	4.08	0.84	10.07	2.20
Papillary carcinoma	131.55	40.48	459.78	106.26	2.47	0.61	9.45	2.34
Chromophobe carcinoma	138.30	40.58	285.86	70.33	3.42	0.98	8.60	1.98
Oncocytoma	168.14	54.76	289.07	58.89	4.02	1.40	14.37	3.48

where: SD is standard deviation of the mean, MVD is microvascular density, MVA is microvascular area

TABLE 5
Values of minimal spanning tree parameters

	Mean	Min	Max	SD
MSTmean	60.26	33.46	114.94	16.33
MSTsd	33.02	12.18	84.99	14.42
MSTmax	303.19	118.21	672.46	124.63
MSTmin	8.52	2.52	13.42	1.94
MSTsum	116852.32	29974.53	324657.70	68669.90

where: SD is standard deviation of the mean, MST is the minimum spanning tree, MSTsum is the sum of the lengths of the MST edges, MSTmean is the mean of the lengths of the MST edges, MSTsd is standard deviation of the lengths of the MST edges, MSTmin is the minimum of the lengths of the MST edges, MSTmax is the maximum of the lengths of the MST edges.

TABLE 6
Means of minimal spanning tree parameters by histologic diagnoses

	MSTmean	MSTsd	MSTmax	MSTmin	MSTsumt
Clear Cell carcinoma	57.67	31.62	316.35	8.37	124514.96
Papillary carcinoma	72.51	42.33	335.80	8.24	120007.34
Chromophobe carcinoma	62.36	33.70	253.18	9.05	89429.69
Oncocytoma	56.06	28.21	284.65	8.73	123423.70

where: MST is the minimum spanning tree, MSTsum is the sum of the lengths of the MST edges, MSTmean is the mean of the lengths of the MST edges, MSTsd is standard deviation of the lengths of the MST edges, MSTmin is the minimum of the lengths of the MST edges, MSTmax is the maximum of the lengths of the MST edges.

TABLE 7
Fractal dimension of the vessels by histologic types

	Mean	Min	Max
Clear Cell carcinoma	1.32	1.00	1.62
Papillary carcinoma	1.34	1.06	1.60
Chromophobe carcinoma	1.31	1.05	1.58
Oncocytoma	1.33	1.07	1.60

presented in Table 2. The stages of the tumors were pT1a in 31 cases (19.14%), pT1b in 42 cases (25.93%), pT2 in 21 cases (12.96%), pT3a in 54 cases (33.33%), pT3b in 12 cases (7.41%), pT3c in 1 case (0.62%) and pT4 in 1 case (0.62%). In 3 cases (one papillary and one chromophobe carcinoma), the histological reports were not sufficient for ascribing a pT stage. The mean diameter of the tumor was 6.59cm, (range 1 to 15cm, SD 3.14). In one case of clear cell carcinoma, local lymph node metastases were present. The differences in size and stage between specific diag-

TABLE 8
TMA immunohistochemistry by histologic types

	VEGF-A		GLUT1		Ki67	
	mean	SD	mean	SD	mean	SD
Clear Cell carcinoma	1.17	0.87	0.43	0.55	11.82	28.79
Papillary carcinoma	0.97	0.83	0.17	0.30	8.11	15.85
Chromophobe carcinoma	0.87	0.55	0.09	0.23	1.14	1.52
Oncocytoma	0.79	0.50	0.04	0.12	1.27	2.42

where: SD is standard deviation

noses were not statistically significant. The Fuhrman grade was G-1 in 32 cases (21.33%), G-2 in 71 cases (47.33%), G-3 in 33 cases (22.00%), G-4 in 14 cases (9.33%). Oncocytomas were not graded.

The mean values for individual vessels were as follows: area 224.66 μm^2, SD 589.64, minimum diameter 12.56 μm, SD 8.86, maximum diameter 27.74 μm, SD 23.12, perimeter 79.75 μm, SD 91.12, SF 0.49 SD 0.22 and ellipticity 2.61 SD 1.56. The values of these parameters by histologic types are shown in Table 3. Of note are the quite high standard deviations of the size parameters, as both single endothelial cells and large vessels were included. For all the parameters under study, the differences between diagnostic categories were statistically significant; on post-hoc analysis there were differences between all individual types. The discriminant function analysis was applied to check a possibility of classifying the tumors according to the characteristics of individual vessels. However, the performance of the constructed models was poor, with the best being able to satisfactorily classify 65% of clear cell carcinomas, none of other tumors.

The mean MVD was 163.62 (range 40.48 to 489.18 SD 91.30). The mean MVA was 3.75 (range 0.61 to 14.37 SD 2.36). The values of these parameters according to diagnoses are shown in Table 4. The differences in both MVA and MVD were statistically significant. On post-hoc analysis, it was due to a difference between clear cell and papillary carcinoma. The size of the tumor and vascular density parameters were inversely correlated; the relationship was the strongest for oncocytoma (for MVD r=-0.31 and for MVA r= -0.27) and the weakest for chromophobe carcinoma (for MVD r=-0.02 and for MVA r= -0.06); however, the differences between these correlation coefficients were not statistically significant. The relationship between Fuhrman grade and microvascular parameters was investigated only for the largest group, the clear cell carcinomas. The mean MVD was 202.75 for G-1 tumors, 194.53 for G-2 tumors, 150.22 for G-3 tumors and 113.96 for G-4 tumors. The differences were statistically significant and the correlation coefficient R= -0.29. The mean MVA was 4.12 for G-1 tumors, 4.51 for G-2 tumors, 3.71 for G-3 tumors and 2.70 for G-4 tumors. The differences were statistically significant and the correlation coefficient R= -0.20.

The values extracted from the minimum spanning tree are presented in Table 5 and their mean values by diagnoses in Table 6. Significant differences were seen between histologic types in MSTmean, MSTsd, and MSTsum. On post-hoc analysis, the differences in MSTmean depended on the difference between clear cell and papillary carcinoma, the MSTsd difference was found to be dependent on the difference between clear cell and papillary carcinomas and between oncocytoma and papillary carcinomas, and the MSTsum difference was noted to be dependent on the difference between clear cell and chromophobe carcinomas.

The mean fractal dimension was 1.32 (range 1.00 to 1.62). The fractal dimensions of the vessels according to diagnoses are shown in Table 7 (standard deviations are all 0.07). Although some differences are visible, they are not statistically significant (on one-way ANOVA $p<0.062$).

On immunohistochemistry, the mean index of VEGF-A staining was 1.05 (SD 0.79); the mean index of GLUT-1 staining was 0.30 (SD 0.48); the mean index of Ki67 staining was 8.30 (SD 23.24). The values of indexes for individual histologic diagnoses are shown in Table 8. On Kruskal-Wallis ANOVA, the differences were significant for all but VEGF-A staining. On post hoc analysis, the GLUT-1 staining was different between clear cell versus chromophobe carcinomas and oncocytomas; the Ki67 index was different between clear cell carcinomas and oncocytomas, and to a lesser degree between clear cell and chromophobe carcinomas ($p<0.071$). The results of the immunohistochemical staining were correlated with morphological and vascular parameters in specific histologic types. The strongest correlations were seen 1) for clear cell carcinoma between the Fuhrman grade and Ki67 index (R=0.32), Fuhrman grade and VEGF-A (R= -0.23), mean vessel area and GLUT-1 (R=0.29); 2) for papillary carcinoma between the tumor diameter and VEGF-A (R=0.28), GLUT-1 and Fuhrman grade (R=0.38), Ki67 and mean area of vessel profile (R=0.53) ; 3) for oncocytoma between MSTmax, MSTmin

and VEGF-A expression (R=0.69 and R=0.59), GLUT-1 and MVD (R= -0.29), Ki67 and tumor diameter (R= -0.45); 4) for chromophobe carcinoma between VEGF-A and MSTsum (R=0.28), GLUT-1 and MSTsum (R= -0.35) and between Ki67 and MSTmin (R=0.30).

In summary, we were able to show that the epithelial renal tumors have important differences in the intensity and structure of their vasculature.

Discussion

The main categories of kidney tumors are conventional (clear cell) carcinoma, chromophobe renal cell carcinoma, papillary carcinoma and oncocytoma [9]. Differences in the genetic background of carcinoma types are becoming increasingly important, as new, specific treatment modalities are introduced [31]. The pathogenesis of conventional (clear cell) renal carcinoma is best known. It is thought that the sporadic cases share the same basic mechanism with von Hippel-Lindau disease. In both cases the VHL gene is inactivated by mutation of the gene itself or methylation of the gene promoter [13, 20, 22]. Such changes are reported in the majority of sporadic and familial cases. The functions of pVHL are not completely understood, but we know that it constitutes a part of the E3 ubiquitin ligase system. This system ubiquitinates several proteins, including hypoxia inducible factor (HIF), marking them for removal. HIF1α and HIF2α are the unstable parts of a transcription regulating systems, inducing, if present, the activity of several genes, including PDGF, bFGF, TGF-α, erythropoietin, carbonic anhydrase IX, GLUT-1 and VEGF-A [17, 26, 28, 33, 39]. VEGF-A induces endothelial cell proliferation, protects them from apoptosis and prolongs survival resulting in new vessel formation [2, 11, 43]. The expression of GLUT1 and HIF1α is positively correlated. GLUT-1 was shown to be correlated with tumor stage in papillary but not in clear cell carcinoma. In all cases, a lower expression of GLUT-1 was a good prognostic sign [30]. As the consequence of the aforementioned mechanism, VEGF-A mRNA is overexpressed in up to 90% of clear cell carcinomas [22, 46]. However, on immunohistochemistry in formalin fixed, paraffin embedded tissue, more than 1/2 tumors may be negative [36, 44]. The recognition of the described pathway leads to development of antiangiogenic agents for treatment of advanced clear cell carcinoma, which have produced promising results in recent trials [10, 14, 35].

The pathogenesis of other types of renal tumors is not related to the VHL gene alterations [24]. In papillary tumors, the basic defect may lay in activating mutation of c-Met. Its product, HGF receptor, has protein kinase activity, with continuous activation leading to cell proliferation [19, 31, 42, 45]. Familial chromophobe renal cell carcinoma of Birt-Hogg-Dube syndrome and a subset of sporadic cases are related to alteration in the HDB gene. Its product, folliculin, participates in mTOR signaling system [25]. The basic effect of other chromophobe renal cell carcinomas was suggested to consist in mutations in c-Kit, the product of which is here overexpressed [49], however, no mutation was detected [18, 37, 38]. The exact role of the hypoxia pathway in non-clear cell carcinomas is unknown. On the other hand, it is obvious that angiogenesis is involved in non-clear cell tumor formation and development, as in any other cancer. In fact, some response to Sunitinib in papillary and chromophobe carcinoma was observed recently by Choueiri et al. [5].

Formation of vessels depends on several factors and mechanisms [4, 21]. Besides the best known endothelial sprouting, various alternative vascularization mechanisms in cancer were described, including vessel co-option, intussusceptive microvascular growth and glomeruloid angiogenesis [8, 21]. The underling mechanisms are far from clear, their role in cancer remains poorly understood and in particular there are no data on their role in renal carcinoma. Interestingly, the intussusceptive microvascular growth was shown to be induced by erythropoietin, at least in the animal model [6], and erythropoietin is one of the substances enhanced by the hypoxia pathway [26]. On the other hand, VEGF was shown to be involved mainly in sprouting angiogenesis [12].

To detect small vessels, immunohistochemical reactions to endothelial cell antigens are used. Many antibodies are commercially available, may mark different subsets of vessels and have been used in renal cell carcinoma [7, 23, 29, 34, 48]. We were reluctant to use vWF as it may stain a subset of vessels only. Although CD31 is usually preferred for vessel staining, we chose CD34 immunohistochemistry, because strong and very constant reaction permitted an easy use of automatic segmentation, which was of prime importance for this work. 'Disturbing' CD34+ cells, such as fibrocytes or hematopoietic cells were not prevalent in renal carcinoma, as seen in piloting stains (data not shown). Interestingly, in Yilmazer et al. study, only CD34-positive, but not CD31-positive vessel count was correlated with other parameters [50].

The method most extensively used in assessing microvessel density was searching for the area with most prominent vascularization ('hot spot') and counting vessels manually under the microscope [15, 32]. Automatic image analysis was used by some authors. Mertz et al. [34] developed an automatic image analysis system for quantify-

ing CD34 stained vessels of renal carcinoma. The authors employed a set of fluorescence dyes, which allowed for easy segmentation. As it was shown in the present paper, a similar analysis may be performed using a much simpler immunohistochemistry-based protocol.

The values of microvascular density and relative vascular area obtained by other authors are broadly similar to these obtained in the present study. MacLennan et al. found MVD in the range 21.6 to 1078.2/mm^2 [32]. Lee et al. [29] obtained the MVD range of 19.3 to 315 and MVA range of 0.7 to 17.9%. Delahunt found the MVD range of 6.8 to 1639.1/mm^2 and MVA range of 1.2 to 60.8% [7]. In Baldewijns et al. work [1], the MVD values for low grade renal carcinoma were 44.22 to 481.8 and for higher grade tumors -27.6 to 439.8. Mertz et al. [34] found MVD in the range of 6 to 987/mm^2 and the MVA range of 0 to 30.3%.

The relationship between vessel density, tumor grade, stage and survival in renal carcinoma in many rapports are discordant. In particular, in some publications, in very contrast to other entities, renal carcinoma appeared to be less aggressive if containing more microvessels. The data on the mechanisms and significance of microvascular density in renal carcinoma is largely limited to the clear cell type, however.

MacLennan et al. [32] found neither correlation between MVD and stage or grade, nor any prognostic significance of vessel density. Gelb et al. saw no difference in survival in of patients with localized clear cell carcinoma in relation to differences in microvessel density [16]. Lee et al. [29] saw a relationship of survival with stage and grade of renal carcinoma, but not with vascular parameters. Mertz et al. [34] found that MVA may have a prognostic value not if used as a continuous variable, but only if the cut-point of 4% and 14% was employed. If so, the patients with higher vascular area survived significantly longer than the ones with lower vascularity. However, on multivariate analysis, only the metastatic status and presence of sarcomatoid features were significantly related to prognosis. Kirkali et al. [27] found the vascular density to be correlated with survival and the rate of metastasis formation. This effect was not related to other prognostic factors, such as stage or nuclear grade. However, on multivariate analysis, only TNM stage and proliferative activity were independent prognostic factors. In Delahunt et al. paper [7], the 5-year survival of patients with <40vessels per a high power field was 39%, but it was 64% for tumors with >40vessels per a high power field. The vascular parameters were, however, dependent on tumor stage and their prognostic significance limited to stage 3 tumors. Sabo et al. [41] analyzed vascular density and vascular fractal dimension in clear cell renal carcinoma. On multivariate analysis, they found that vascular fractal dimension is the only parameter related to the extent of tumor necrosis, which by itself was the only independent prognostic factor in their study. Fractal dimension was higher in low grade tumors, as was the microvessel density. Baldewijns et al. found that renal carcinomas of higher grade show lower MVD, but more intense endothelial cell proliferation and VEGF expression [1]. These authors observed higher indexes of vessel maturation in lower grade tumors. Yagasaki et al. [48] found MVD to be correlated with survival in renal carcinoma. It was also independent of nuclear grade and an independent prognostic factor on multivariate analysis.

Recently, new treatment modalities have been introduced acting on the signaling system participating in angiogenesis [14]. Some of the reports show a quite good response in clear cell renal carcinoma, and therapeutic possibilities in other tumor types are considered. Thus, recognition of the vasculogenic mechanisms in renal cell carcinoma has become of prime importance.

Acknowledgments: The authors would like to thank Mrs. Anna Zysk for excellent technical assistance

References

1. *Baldewijns MM, Thijssen VL, Van den Eynden GG, Van Laere SJ et al:* High-grade clear cell renal cell carcinoma has a higher angiogenic activity than low-grade renal cell carcinoma based on histomorphological quantification and qRT-PCR mRNA expression profile. Br J Cancer 2007, 96, 1888-1895.
2. *Banks RE, Craven RA, Harnden P, Madaan S et al:* Key clinical issues in renal cancer: a challenge for proteomics. World J Urol 2007, 25, 537-556.
3. *Burri PH, Hlushchuk R, Djonov V:* Intussusceptive angiogenesis: its emergence, its characteristics, and its significanc. Dev Dyn 2004, 231, 474-488.
4. *Carmeliet P, Jain RK:* Angiogenesis in cancer and other diseases. Nature 2000, 407, 249-257.
5. *Choueiri TK, Plantade A, Elson P, Negrier S et al:* Efficacy of sunitinib and sorafenib in metastatic papillary and chromophobe renal cell carcinoma. J Clin Oncol 2008, 26, 127-131.
6. *Crivellato E, Nico B, Vacca A, Djonov V et al:* Recombinant human erythropoietin induces intussusceptive microvascular growth in vivo. Leukemia 2004, 18, 331-336.
7. *Delahunt B, Bethwaite PB, Thornton A:* Prognostic significance of microscopic vascularity for clear cell renal cell carcinoma. Br J Urol 1997, 80, 401-404.
8. *Döme B, Hendrix MJC, Paku S, Tóvári J et al:* Alternative vascularization mechanisms in cancer: Pathology and therapeutic implicati. Am J Pathol 2007, 170, 1-15.
9. *Eble JN, Sauter G, Epstein JI:* Tumours of the kidney. In: Eble JN, Sauter G, Epstein JI Eds: WHO Classification of Tumours: Pathology and Genetics of Tumours of the Urinary System and Male Genital Organs (World Health Organization Classification of Tumours) 2004, 9-88.

10. *Escudier B, Pluzanska A, Koralewski P, Ravaud A et al:* Bevacizumab plus interferon alfa-2a for treatment of metastatic renal cell carcinoma: a randomised, double-blind phase III trial. Lancet 2007, 370, 2103-2111.
11. *Ferrara N:* Vascular endothelial growth factor and the regulation of angiogenesis. Recent Prog Horm Res 2000, 55, 15-35, discussion 35-36.
12. *Fujimoto A, Onodera H, Mori A, Isobe N et al:* Vascular endothelial growth factor reduces mural cell coverage of endothelial cells. Int J Exp Pathol 2004, 85, 355-364.
13. *Gallou C, Joly D, Mejean A, Staroz F et al:* Mutations of the VHL gene in sporadic renal cell carcinoma: definition of a risk factor for VHL patients to develop an RCC. Hum Mutat 1999, 13, 464-475.
14. *Garcia JA, Rini BI:* Recent progress in the management of advanced renal cell carcinoma. CA Cancer J Clin 2007, 57, 112-125.
15. *Gelb AB:* Renal cell carcinoma: current prognostic factors. Union Internationale Contre le Cancer (UICC) and the American Joint Committee on Cancer (AJCC). Cancer 1997, 80, 981-986.
16. *Gelb AB, Sudilovsky D, Wu CD, Weiss LM et al:* Appraisal of intratumoral microvessel density, MIB-1 score, DNA content, and p53 protein expression as prognostic indicators in patients with locally confined renal cell carcinoma. Cancer 1997, 80, 1768-1775.
17. *Gunaratnam L, Morley M, Franovic A, de Paulsen N et al:* Hypoxia inducible factor activates the transforming growth factor-alpha/epidermal growth factor receptor growth stimulatory pathway in VHL(-/-) renal cell carcinoma cells. J Biol Chem 2003, 278, 44966-44974.
18. *Haitel A, Susani M, Wick N, Mazal PR et al:* c-kit overexpression in chromophobe renal cell carcinoma is not associated with c-kit mutation of exons 9 and 11. Am J Surg Pathol 2005, 29, 842.
19. *Henke R, Erbersdobler A:* Numerical chromosomal aberrations in papillary renal cortical tumors: relationship with histopathologic features. Virchows Arch 2002, 440, 604-609.
20. *Herman JG, Latif F, Weng Y, Lerman MI et al:* Silencing of the VHL tumor-suppressor gene by DNA methylation in renal carcinoma. Proc Natl Acad Sci U S A 1994, 91, 9700-9704.
21. *Hillen F, Griffioen AW:* Tumour vascularization: sprouting angiogenesis and beyond. Cancer Metastasis Rev 2007, 26, 489-502.
22. *Igarashi H, Esumi M, Ishida H, Okada K:* Vascular endothelial growth factor overexpression is correlated with von Hippel-Lindau tumor suppressor gene inactivation in patients with sporadic renal cell carcinoma. Cancer 2002, 95, 47-53.
23. *Kavantzas N, Paraskevakou H, Tseleni-Balafouta S, Aroni K et al:* Association between microvessel density and histologic grade in renal cell carcinomas. Pathol Oncol Res 2007, 13, 145-148.
24. *Kenck C, Wilhelm M, Bugert P, Staehler G et al:* Mutation of the VHL gene is associated exclusively with the development of non-papillary renal cell carcinomas. J Pathol 1996, 179, 157-161.
25. *Khoo SK, Kahnoski K, Sugimura J, Petillo D et al:* Inactivation of BHD in sporadic renal tumors. Cancer Res 2003, 63, 4583-4587.
26. *Kim WY, Kaelin WG:* Role of VHL gene mutation in human cancer. J Clin Oncol 2004, 22, 4991-5004.
27. *Kirkali Z, Yorukoglu K, Ozkara E, Kazimoglu H et al:* Proliferative activity, angiogenesis and nuclear morphometry in renal cell carcinoma. Int J Urol 2001, 8, 697-703.
28. *Kondo K, Klco J, Nakamura E, Lechpammer M et al:* Inhibition of HIF is necessary for tumor suppression by the von Hippel-Lindau protein. Cancer Cell 2002, 1, 237-246.
29. *Lee JS, Jung JJ, Kim J:* Quantification of angiogenesis by a computerized image analysis system in renal cell carcinoma. Anal Quant Cytol Histol 2000, 22, 469-474.
30. *Lidgren A, Bergh A, Grankvist K, Rasmuson T et al:* Glucose transporter-1 expression in renal cell carcinoma and its correlation with hypoxia inducible factor-1alpha. BJU Int 2007, 101, 480-484.
31. *Linehan WM, Vasselli J, Srinivasan R, Walther MM et al:* Genetic basis of cancer of the kidney: disease-specific approaches to therapy. Clin Cancer Res 2004, 10, 6282S-6289S.
32. *MacLennan GT, Bostwick DG:* Microvessel density in renal cell carcinoma: lack of prognostic significance. Urology 1995, 46, 27-30.
33. *Maxwell PH, Wiesener MS, Chang GW, Clifford SC et al:* The tumour suppressor protein VHL targets hypoxia-inducible factors for oxygen-dependent proteolysis. Nature 1999, 399, 271-275.
34. *Mertz KD, Demichelis F, Kim R, Schraml P et al:* Automated immunofluorescence analysis defines microvessel area as a prognostic parameter in clear cell renal cell cancer. Hum Pathol 2007, 38, 1454-1462.
35. *Motzer RJ, Michaelson MD, Rosenberg J, Bukowski RM et al:* Sunitinib efficacy against advanced renal cell carcinoma. J Urol 2007, 178, 1883-1887.
36. *Paradis V, Lagha NB, Zeimoura L, Blanchet P et al:* Expression of vascular endothelial growth factor in renal cell carcinomas. Virchows Arch 2000, 436, 351-356.
37. *Petit A, Castillo M, Mellado B, Mallofre C:* c-kit overexpression in chromophobe renal cell carcinoma is not associated with c-kit mutation of exons 9 and 11. Am J Surg Pathol 2005, 29, 1544-1545.
38. *Petit A, Castillo M, Santos M, Mellado B et al:* KIT expression in chromophobe renal cell carcinoma: comparative immunohistochemical analysis of KIT expression in different renal cell neoplasms. Am J Surg Pathol 2004, 28, 676-678.
39. *Rini BI, Small EJ:* Biology and clinical development of vascular endothelial growth factor-targeted therapy in renal cell carcinoma. J Clin Oncol 2005, 23, 1028-1043.
40. *Rudzki Z, Kawa R, Okoń K, Szczygieł E et al:* Objective, planimetry-based assessment of megakaryocyte histological pictures in Philadelphia-chromosome-negative chronic myeloproliferative disorders: a perspective for a valuable adjunct diagnostic tool. Virchows Arch 2006, 448, 59-67.
41. *Sabo E, Boltenko A, Sova Y, Stein A et al:* Microscopic analysis and significance of vascular architectural complexity in renal cell carcinoma. Clin Cancer Res 2001, 7, 533-537.
42. *Schmidt LS, Nickerson ML, Angeloni D, Glenn GM et al:* Early onset hereditary papillary renal carcinoma: germline missense mutations in the tyrosine kinase domain of the met proto-oncogene. J Urol 2004, 172, 1256-1261.
43. *Schraml P, Struckmann K, Hatz F, Sonnet S et al:* VHL mutations and their correlation with tumour cell proliferation, microvessel density, and patient prognosis in clear cell renal cell carcinoma. J Pathol 2002, 196, 186-193.
44. *Song KH, Song J, Jeong GB, Kim JM et al:* Vascular endothelial growth factor - its relation to neovascularization

and their significance as prognostic factors in renal cell carcinoma. Yonsei Med J 2001, 42, 539-546.
45. *Sweeney P, El-Naggar AK, Lin S, Pisters LL:* Biological significance of c-met over expression in papillary renal cell carcinoma. J Urol 2002, 168, 51-55.
46. *Takahashi A, Sasaki H, Kim SJ, Tobisu K et al:* Markedly increased amounts of messenger RNAs for vascular endothelial growth factor and placenta growth factor in renal cell carcinoma associated with angiogenesis. Cancer Res 1994, 54, 4233-4237.
47. *Whitney VKM:* Algorithm 422 minimal spanning tree. Commun Assoc Comput Mach 1972, 15, 273-274.
48. *Yagasaki H, Kawata N, Takimoto Y, Nemoto N:* Histopathological analysis of angiogenic factors in renal cell carcinoma. Int J Urol 2003, 10, 220-227.
49. *Yamazaki K, Sakamoto M, Ohta T, Kanai Y et al:* Overexpression of KIT in chromophobe renal cell carcinoma. Oncogene 2003, 22, 847-852.
50. *Yilmazer D, Han U, Onal B:* A comparison of the vascular density of VEGF expression with microvascular density determined with CD34 and CD31 staining and conventional prognostic markers in renal cell carcinoma. Int Urol Nephrol 2007, 39, 691-698.

Address for correspondence and reprint requests to:
Dr Krzysztof Okoń
Department of Pathomorphology Collegium Medicum,
Jagiellonian University
Ul. Grzegórzecka 16
31-531 Kraków